Micromorphology of Macromolecular Superabsorbent Polymer and its Fractal Characteristics

Li Yunkai,[1,2] Xu Tingwu,[3] Ouyang Zhiyun,[2] Lin Xiongcai,[1] Liu Honglu,[4] Hao Zhongyong,[4] Yang Peiling[1]

[1]*Center for Agricultural Water Research in China, Water-Saving and Irrigation, China Agricultural University, Beijing 100083, China*
[2]*National Key Laboratory of Urban and Regional Ecology, Ecological Environment Research Center, The Group of Urban and Industrial Ecology, China Academy of Sciences, Beijing 100085, China*
[3]*International College at Beijing, English Education, China Agricultural University, Beijing 100083, China*
[4]*Beijing Hydraulic Research Institute, Beijing 100044, China*

Received 21 October 2008; accepted 14 February 2009
DOI 10.1002/app.30323
Published online 8 May 2009 in Wiley InterScience (www.interscience.wiley.com).

ABSTRACT: Superabsorbent polymer (SAP) can absorb a solution of 10-folds to 1000-folds as much as its own weight. Its micromorphology directly affects its water absorption mechanism and absorption characteristics. In this work, we selected three types of polymer products for research analysis: KH (sodium polyacrylate-type), HLM (polyacrylamide-type), and AS (polyacrylamide-kalium-crylic acid-crosslinking-copolymer-type). The environmental scanning electronic microscope (ESEM) method and the fractal theory are applied for studying the micromorphology of the three types of SAPs. The results show that KH possesses the highest water absorption multiplying factor and HLM possesses the lowest one. Under the condition of repeated water absorption and water release, the structure of HLM hydrogel transfers from gridding membrane to network structure. Various types of cation solutions significantly affect the characteristics of micromorphology of HLM hydrogel, and both uniqueness and diversity prevail. Under the condition of repeated water absorption and water release, the swelling multiplying factor of HLM in deionized water abides by an "inverted U" distribution. The water absorption multiplying factor for the third time is the largest one. This is primarily caused by both reduction of resilience of crosslinking network and dissolution of polymer on the surface of hydrogel under the condition of repeated water absorption and water release. The boundary of hydrogel pore network of the three types of SAPs possesses fractal characteristics. The number of fractal dimensions is as follows: fractal dimension of HLM $<$ fractal dimension of AS $<$ fractal dimension of KH. With the increase of the number of repeated water absorption and water release, the number of fractal dimensions of cross-sectional pore boundary reduces, that is, T1 (1.3848) $>$ T3 (1.2100) $>$ T5 (1.1226). © 2009 Wiley Periodicals, Inc. J Appl Polym Sci 113: 3510–3519, 2009

Key words: macromolecular SAP; water absorption; micromorphology; structure; fractal

INTRODUCTION

Superabsorbent polymer (SAP) is one new type of functional macromolecular material widely used in agriculture, forestry, construction, sanitation, biology, national defense, medical science, etc., because it can absorb a solution of 10-folds to 1000-folds as much as its own weight.[1] The characteristics and theory about its water absorption and water retention have drawn much attention from many researchers, manufacturers, and users. The absorption primarily relies on the three-dimensional networks of SAP to store abundant free water.[2–4] Water absorption capacity of SAP is decided by both extension caused by ionic charge repulsion of macromolecular electrolyte and expansion resistance caused by crosslinking structure and hydrogen bond. The internal micromorphology of SAP directly affects its absorption mechanism and absorption characteristics.[5,6]

Microtechnique is commonly used in observing material configuration and physical structure, especially the electronic microscope technique. The ordinary scanning electronic microscope (SEM) can be used in observing dry samples of SAP[7,8]; Hydrogel can be observed by SEM after completion of sample preparation in tissue desiccator at a temperature of –

Correspondence to: L. Yunkai (liyunkai@126.com) or Y. Peiling (yangpeiling@126.com).

Li Yunkai, Xu Tingwu, Ouyang Zhiyun and Lin Xiongcai equally contributed to this paper.

Contract grant sponsor: Program for Changjiang Scholars and Innovative Research Team in University (PCSIRT); contract grant number: IRT0657.
Contract grant sponsor: "11th Five-Year" Key Project of Beijing; contract grant number: Ho10710240113.
Contract grant sponsor: Science Fund of China Postdoctor; contract grant number: 20080430072.
Contract grant sponsor: Program for Beijing Key Subject of Hydrology and Water Resources.

60°C. SEM can also be used for observing dilated and repeatedly freeze-dried SAP in liquid nitrogen. Environmental scanning electronic microscope (ESEM) is convenient for observing water-contained samples and it can eliminate the problem of sample transfiguration because of microtherm and refrigeration and it can better reflect the practical structure of water-contained samples.[9] Generally speaking, most observations are limited to observe the superficial morphology of the macromolecular network structure of dry gel particles. Much less research is related to the observation of micromorphology of hydrogel. No research has been reported in micromorphology change after repeated water absorption and water release and in ionic solution as well as the influence on characteristics of water absorption and water retention.

Fractal theory can help people deal with various irregular geometric shapes and chaotic phenomena from new perspectives. Fractal theory has become a powerful tool to explore irregular structures and configurations. Sporadic researches have been reported on the application of fractal theory in macromolecular science during recent years.[3,10] With application of fractal theory in researches and development of environmental scanning microscopes and image analysis techniques, theoretical analysis methods and technical measures are provided for describing the internal structure of SAP hydrogel. Hence, in this work, three types of widely used SAP are selected for the research. ESEM and fractal theory are used to test and analyze characteristics of internal micromorphology of dry gel particles, hydrogel after repeated water absorption and water release as well as hydrogel in different ionic solutions. This article aims at providing reference frame for exploring water absorption mechanism of SAP and enhancing its property.

MATERIALS AND METHODS

Experimental materials

Three polymer products of KH (sodium polyacrylate-type), HLM (polyacrylamide-type), and AS (polyacrylamide-kaliumcrylic acid-crosslinking-copolymer-type) were selected for the experiment. For KH, "KEHAN 98" Type-C SAP produced by KEHAN Polymer (Baoding, Hebei Province) was selected. It is not toxic for crops and it is biodegradable and pH-neutral. Removal of sodium was applied for it. For HLM, the STOCKOSORB-KL polymer produced by Beijing HANLIMIAO Company (Beijing, China) was selected. For AS, the polymer produced by Essen Company, France, was selected. Figure 1 shows the molecular formula of the three products. Samples were prepared by solution aggregation method. The following four size

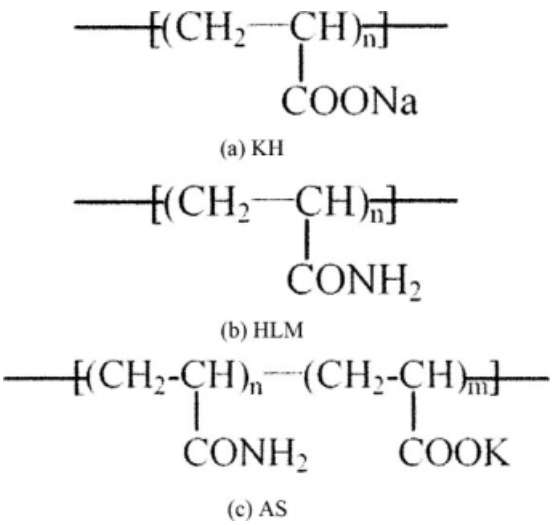

Figure 1 Structural formula of the three types of SAP.

category fractions were sieved: less than 1 mm, 1–2 mm, 2–3 mm, and larger than 3 mm. Particle size of 2–3 mm was used for the experiment.

The chemical agents for the experiment were KCl, NaCl, $CaCl_2$, $FeCl_3$, and $FeCl_2$ manufactured by Beijing Chemical Analysis Company, and the experimental water used was the deionized water manufactured by Beijing Quchen Water Plant.

Experimental method

Swelling characteristic curve

Prepare 0.01 mol L^{-1} $CaCl_2$, $FeCl_3$, $FeCl_2$ solutions and 0.02 mol L^{-1} NaCl and KCl solutions and set deionized water as contrast. Then, add 1.00 g SAP into solutions for swelling and filter at time intervals of 1, 3, and 8 min (every 8 min afterward). Filtering method of 100-mesh was applied.[11] Weigh the mass of SAP hydrogel and obtain water absorption multiplying factors of SAP at different points of time. Formula (1) shows how to calculate the multiplying factors of SAP.

$$S = (W_t - W_d)/W_d \quad (1)$$

where S denotes the multiplying factor; W_t denotes the mass of SAP hydrogel at the moment of t in time; W_d denotes the mass of dry gel of SAP. The experiment stops when the relative water absorption velocity is less than 0.0005 (g g^{-1})/(g g^{-1} min^{-1}). Formula (2) shows how to calculate the relative water absorption velocity:

$$V_{Rt} = (W_{t+1} - W_t)/(\Delta t \times W_t) \quad (2)$$

where V_{Rt} denotes the relative water absorption velocity and Δt denotes the time increment.

Then, add the hydrogel into the culture dish of 120 mm in diameter after reaching swelling equilibrium and place the dish into the oven with a temperature

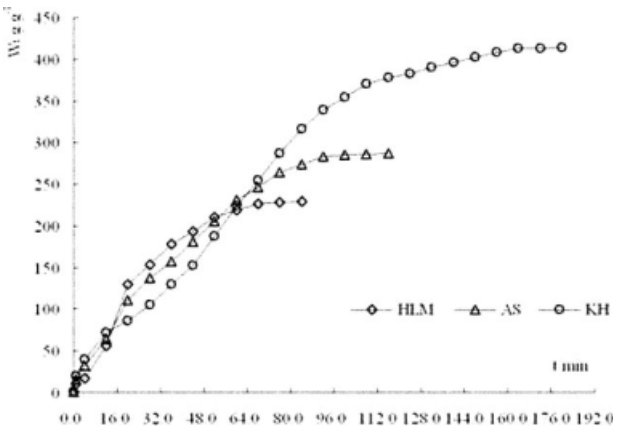

Figure 2 Swelling characteristic curves of the three types of SAP.

of 60°C. Under constant temperature, heat it until the mass of hydrogel reduces to 8.00 ± 0.50 g. Take it out timely to prevent destruction of the network structure. Repeat the process of water absorption, water release, and water absorption for five times.

Scanning internal micromorphology

Use Hitachi S-3500N ESEM and FEI Quanta 200 ESEM for observation. Place the Au layer on dry gel particles of AS and KH and place them on observation platform of FEI Quanta 200 ESEM. Observe the process under high-vacuum condition with an acceleration voltage of 30 kV. Directly scan the dry gel particles of HLM on observation platform of Hitachi S-3500N ESEM with an acceleration voltage of 4.6 kV and vacuum degree of less than 1 Pa. Use a cutting blade to obtain the middle portion of SAP hydrogel and place it on the observation platform of Hitachi S-3500N ESEM for quick scanning and observation. To reduce errors in practical experiment, five test regions on the surface of each sample were chosen at random. Five SEM images were obtained after testing the five regions independently. Because of the existence of problems of unclear contrast and polarized light in obtaining images, each image was transferred into an 8-level grayscale image. Image processing technique was applied in handling the contrast and polarized light problems.

Pore network boundary fractal and its dimension

Fractal geometry deals with substantial unsmoothed and irregular geometric shapes in nature and in nonlinear system and tries to quantitatively describe the complex shapes, which are hard to be described by the classical Euclidean geometry. Fractal dimension quantitatively describes the fractal complexity and it is a characteristic quantity for describing the fractal. The island analysis was used to calculate fractal dimension of pore cross-sectional boundary of internal structure of SAP hydrogel. The island analysis is a method for calculating fractal dimension based on the measurement relationship. Mandelbrot pointed out[12]:

$$\alpha_D(\varepsilon) = \frac{L^{\frac{1}{D}}(\varepsilon)}{A^{\frac{1}{2}}(\varepsilon)} \tag{3}$$

where L denotes the pore perimeter; A denotes the pore area; and D denotes the fractal dimension; $\varepsilon = \eta/L_0$, where η denotes the absolute measurement scale and L_0 denotes the initial perimeter of the image; with constant scale of η, $\alpha_D(\varepsilon)$ is a constant while $\alpha_D(\varepsilon)$ is only related to the selected scale and it is not related to the image size. Take logarithm for both sides of Formula (3) and obtain the following equation:

$$\log L(\varepsilon) = D \log \alpha_D(\varepsilon) + \frac{D}{2} \log A(\varepsilon) = C + \frac{D}{2} \log A(\varepsilon) \tag{4}$$

where C is a constant. Measure the perimeter and area of each pore on microphotograph of SAP hydrogel. The fractal dimension D is twice as large as the slope of the double-log curve between area and perimeter. Use Image-pro Software to test each SEM image after completion of binarization processing, and then calculate the area and perimeter of each pore on each sample surface.

RESULTS AND ANALYSES

Swelling characteristics of SAP

Figure 2 shows the test results of the swelling characteristic curve of HLM, AS, and KH in deionized water by 100-mesh sieving method. Figure 3 shows the swelling characteristic curve of HLM in deionized water after five times of repeated water

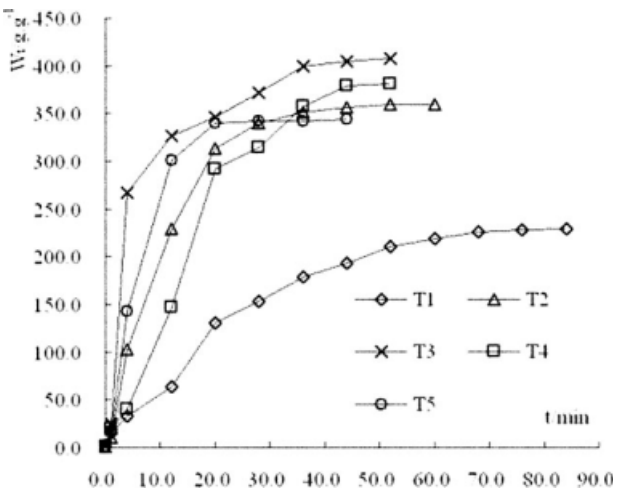

Figure 3 Repeated swelling characteristic curves of HLM.

absorption and water release with notation symbols of T1–T5. Figure 2 indicates that the multiplying factor of KH after reaching equilibrium is the largest (413.9 g g^{-1}), the multiplying factor of AS is smaller (287.4 g g^{-1}), and the multiplying factor of HLM is the smallest (229.2 g g^{-1}). The time for HLM to reach equilibrium is the shortest (84.0 min), the time for AS to reach equilibrium is longer (116.0 min), and the time for KH to reach equilibrium is the longest (180 min). During the initial phase, water absorption velocity of KH is the highest while that of HLM is the lowest. During the middle phase, the sequence is just on the contrary. Figure 3 indicates that the swelling multiplying factor of HLM in deionized water abides by an "inverted U" distribution. The swelling multiplying factor increases over the first three tests and then decreases. However, the swelling multiplying factors for the last four tests are all larger than that of the first test.

Characteristics of micromorphology of dry gel particles and hydrogel

Figure 4 shows the scanning results of micromorphology of dry gel particles and deionized hydrogel of the three types of SAP. Figure 4(a) indicates that the surface of dry gel particles of KH is smooth and there are relatively large pores on it. Figure 4(b) indicates that the surface of dry gel particles of HLM is striated and there are dents among striations. Figure 4(c) indicates that the surface of dry gel particles of AS is extremely irregular. There exist wrinkle phenomena and there is a striation arrangement in some regions. Figure 5(a) indicates that KH hydrogel possesses the classical alveolate crosslinking network structure. The network framework is poly(acrylic acid) and there is an extremely asymmetric distribution of pore sizes. Figure 6 indicates that the striations of dry gel of HLM disappear. Its structure is an alveolate crosslinking gridding membrane structure with various shapes and sizes. The striation structure is expanded into a new structure because of the repulsion of ionic charges. Figure 5(b) indicates that the micromorphology of the AS hydrogel is similar to that of HLM. However, there are many fractures of membranes. Its structure is a transitional one between gridding membrane and network structure.

Figure 6 indicates that there is a strong similarity among images with different magnifications of 100× to 400×. Figure 7 shows the correlation relationship of log A and log L for pore boundaries by applying the image processing technique. There is a strong correlation with R^2 being more than 0.85. The results of fractal dimension of pore network boundary are calculated to be 1.3702, 1.3494, and 1.3848, respectively. The error is less than 2.56%. The consistency is good and there exists a significant scale invariance. The HLM hydrogel possesses fractal characteristics. Figure 8 indicates that AS hydrogel and KH hydrogel also possess fractal characteristics and the fractal dimensions are 1.5242 and 1.6500, respectively.

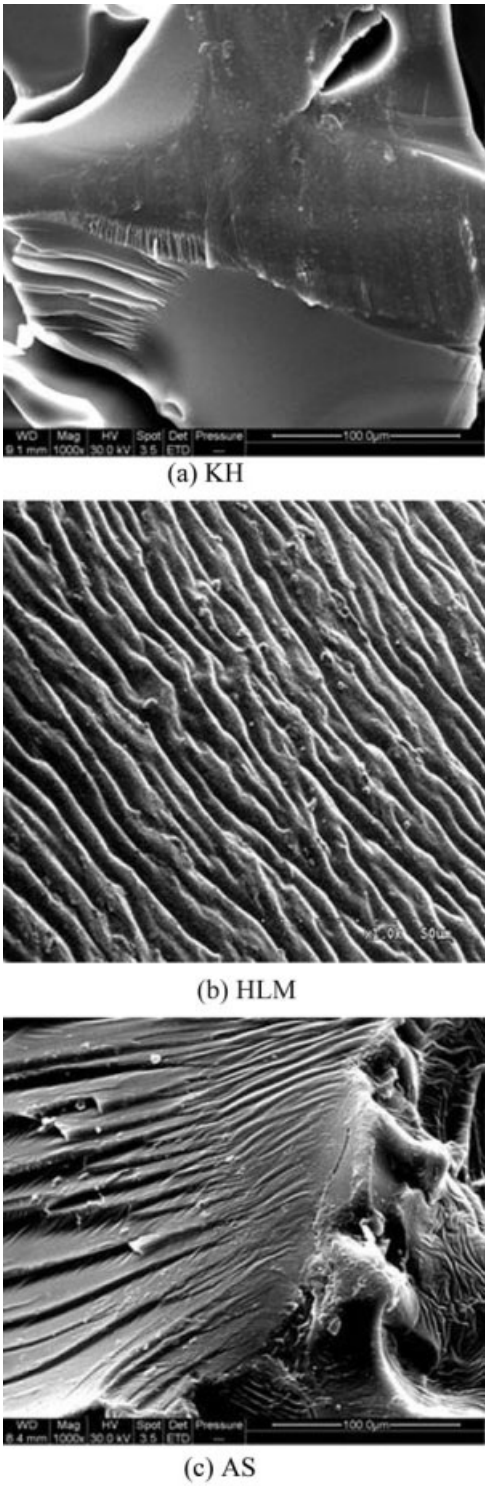

Figure 4 Micromorphology of dry gel particles of SAP.

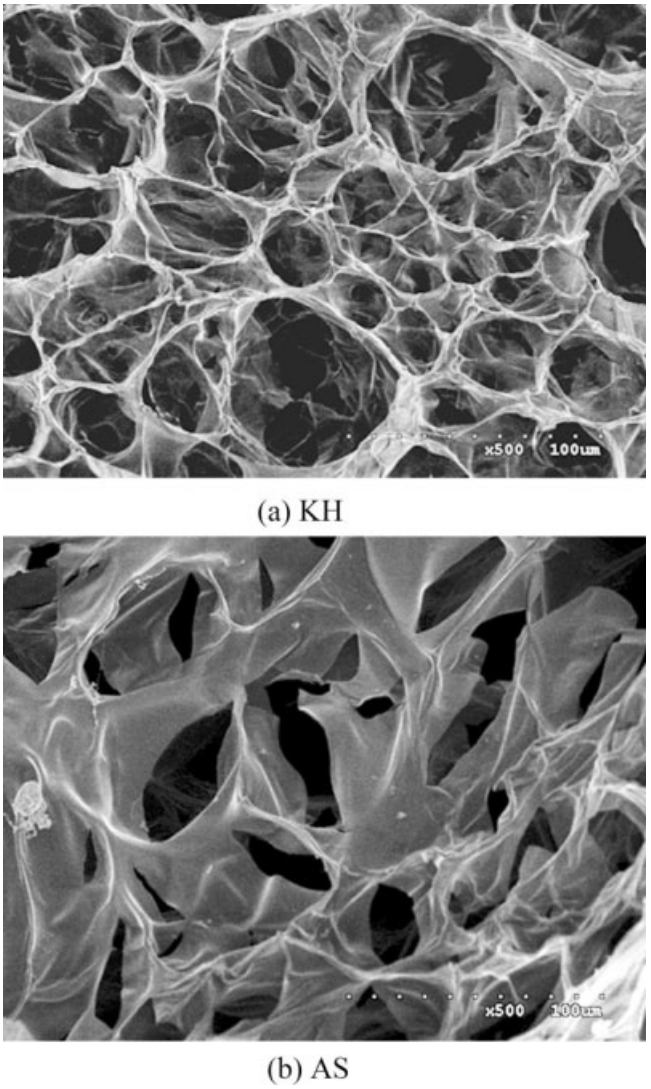

Figure 5 Micromorphology of hydrogel of KH and AS after swelling in deionized water.

Influence on micromorphology of internal structure of hydrogel after repeated water absorption and water release

Figure 9 shows the change in micromorphology of HLM hydrogel after the third and the fifth water absorption and water release. Combined with Figure 6(c), it is shown that all membranes in three-dimensional gridding membrane structure are ruptured and the new structure is a three-dimensional network structure. This indicates that the physical structure of HLM hydrogel transfers from the gridding membrane structure to the network structure. Figure 9 also indicates that water absorption velocity of HLM for the first time is much lower than velocities for other times. There is no significant difference in the water absorption velocities from the second time to the fifth time. This indicates that the membrane structure of HLM has been ruptured for the second water absorption. Figure 10 shows the analytical results for fractal characteristics of pore boundaries on two images. The fractal dimensions for the third time and the fifth time are 1.2100 and 1.1226, respectively, whereas the fractal dimension for the first time is 1.3848. From the perspective of the change in fractal characteristics of hydrogel after

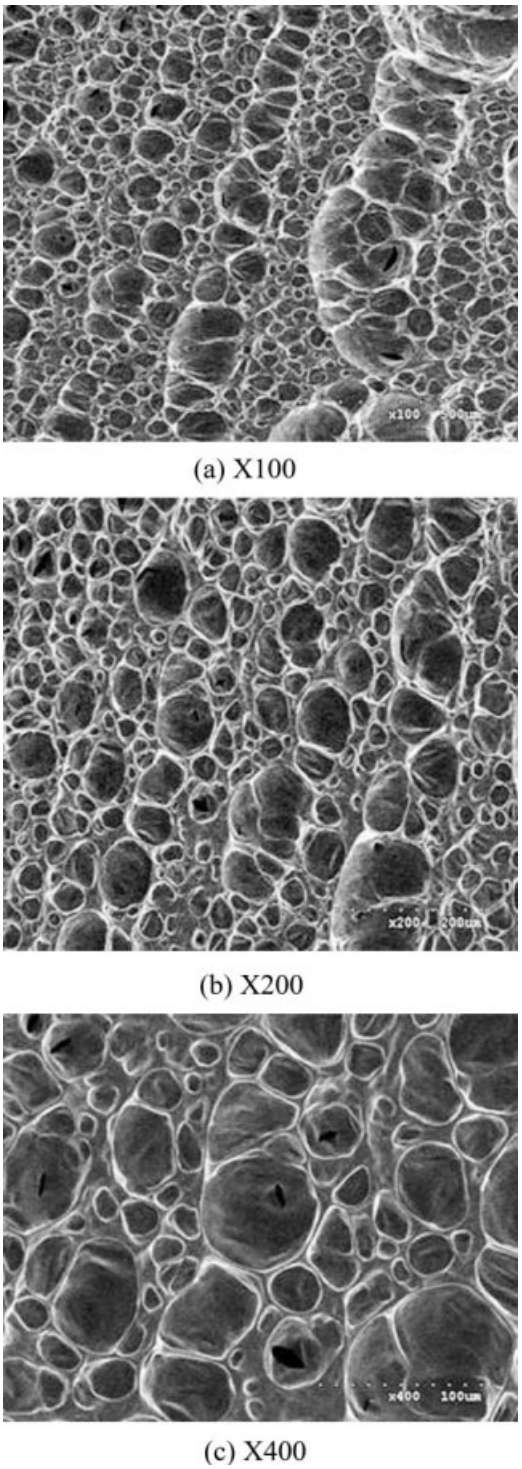

Figure 6 Micromorphology of HLM hydrogel after swelling in deionized water.

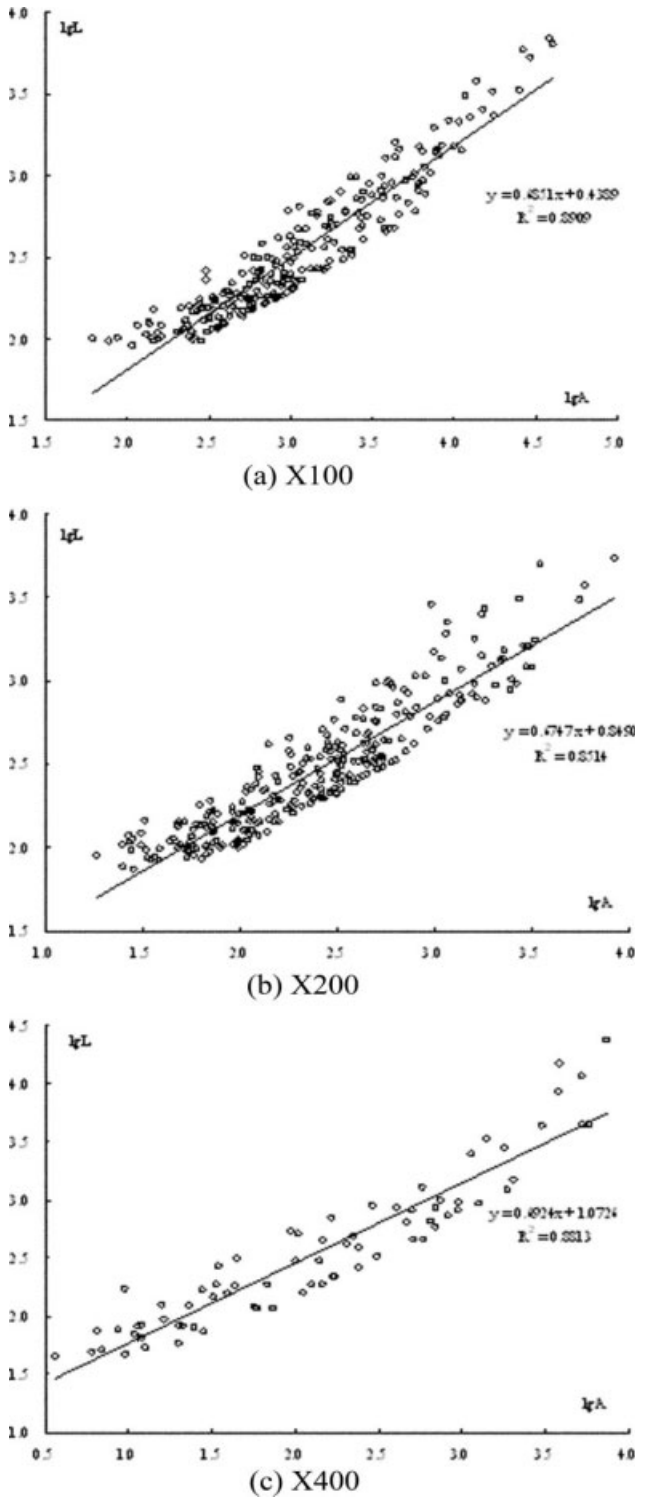

Figure 7 Calculation of fractal dimension of pore boundary of HLM hydrogel.

five times of repeated water absorption and water release, the fractal dimension of cross-sectional pore boundary decreases with respect to increase of times of repeated water absorption and water release.

Influence of cation on internal structure of SAP hydrogel

Figure 11 shows the micromorphology of HLM after its first swelling in cation solutions of Na^+ and K^+. Figure 12 shows the micromorphology of HLM after its first swelling in cation solutions of Ca^{2+}, Fe^{2+}, and Fe^{3+}. The images indicate that the alveolate crosslinking gridding membrane structure and the fractal characteristics for the hydrogel disappear. The five cations have different influences on the micromorphology of hydrogel. There is a clear "wrinkle" phenomenon on Na^+ hydrogel interface [Fig. 11(a)]. There is a clear structural context on K^+ hydrogel interface [Fig. 11(b)] while part of the membrane structure is ruptured and there is a property of self-similarity for its internal structure. The internal membrane structure of Fe^{2+} hydrogel

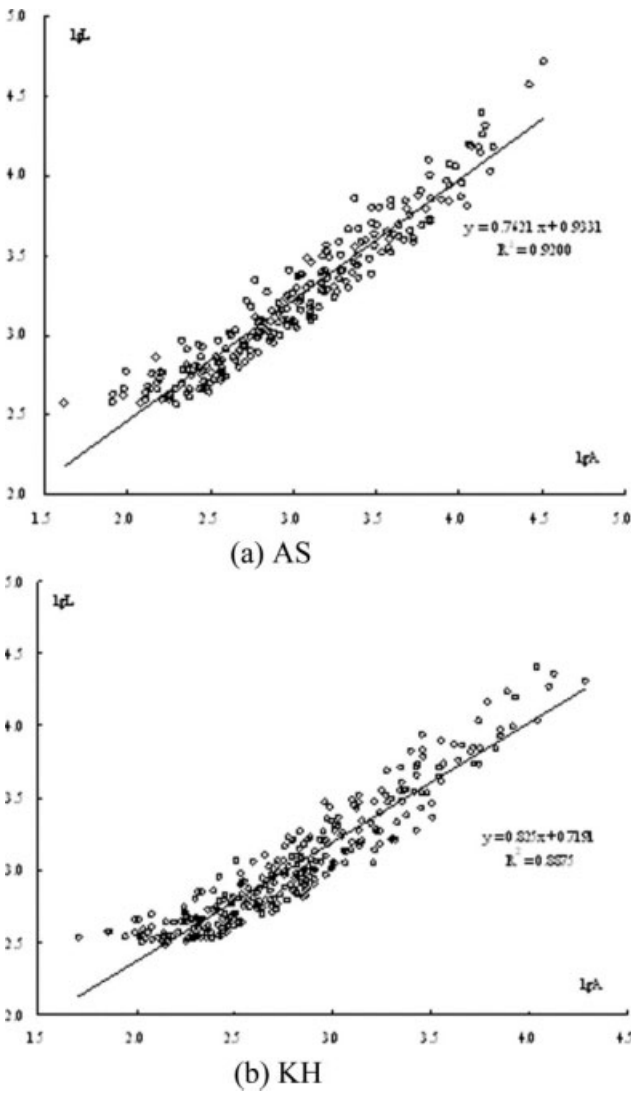

Figure 8 Calculation of fractal dimension of pore boundary of AS hydrogel and KH hydrogel.

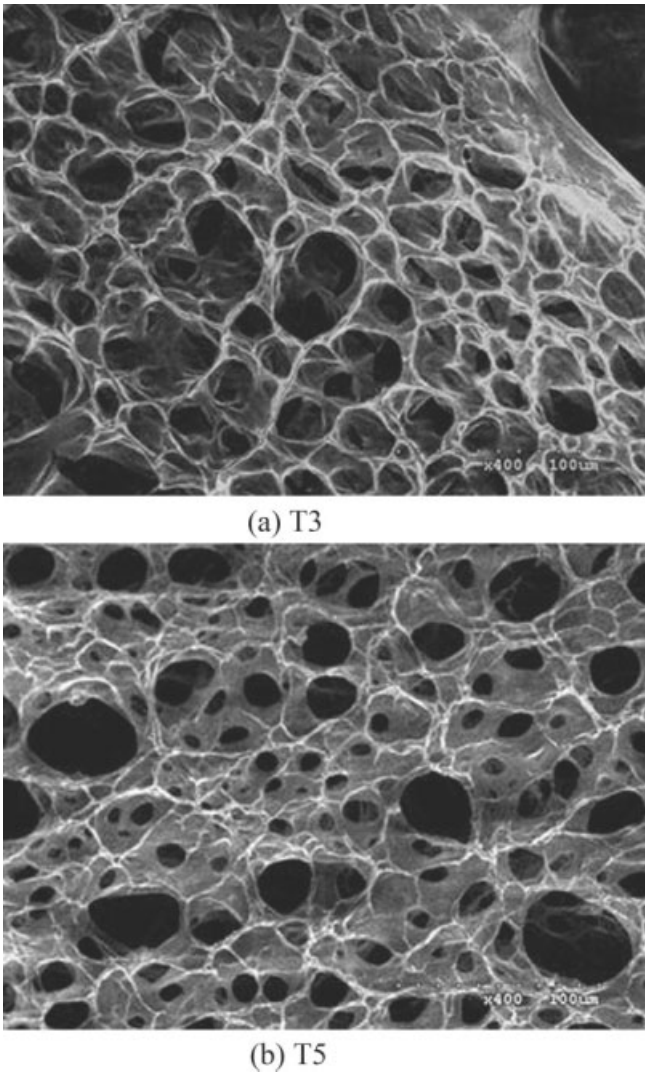

Figure 9 Change in micromorphology of SAP hydrogel after repeated water absorption and water release.

possesses a flocculent distribution [Fig. 12(a)]. There exists an indented phenomenon for Fe^{3+} hydrogel.

DISCUSSIONS

SAP can quickly absorb substantial water of 10-folds to 1000-folds as much as its own weight and then it becomes gelatinous. It has properties of large water absorption capacity, quick water absorption velocity, and strong water retention ability and it is nonpoisonous and tasteless. It is widely used in agricultural gardening, civil construction, food processing, petrochemical engineering, sanitary and medical services, etc.[1,4] It has vast potential for future development. The characteristics and mechanism of its water absorption and water retention have drawn much attention from many researchers, manufacturers, and users, which has become the frontier and hot issues in regions of SAP research.

The mechanism of water absorption of SAP is related to its molecular structure. For the mechanism of water absorption of crosslinking SAP, the ionic network structure theory is currently an accepted theory.[2,3] SAP uses its internal three-dimensional network to store substantial free water. The micromorphology of SAP directly affects its water absorption and water release properties. ESEM method used in this work confirms that KH hydrogel possesses a classical alveolate crosslinking network structure. This result is the same as results obtained by many other researchers. HLM hydrogel possesses a three-dimensional gridding membrane structure, whereas AS hydrogel possesses a transitional structure between network structure and gridding membrane structure. From this point of view, water

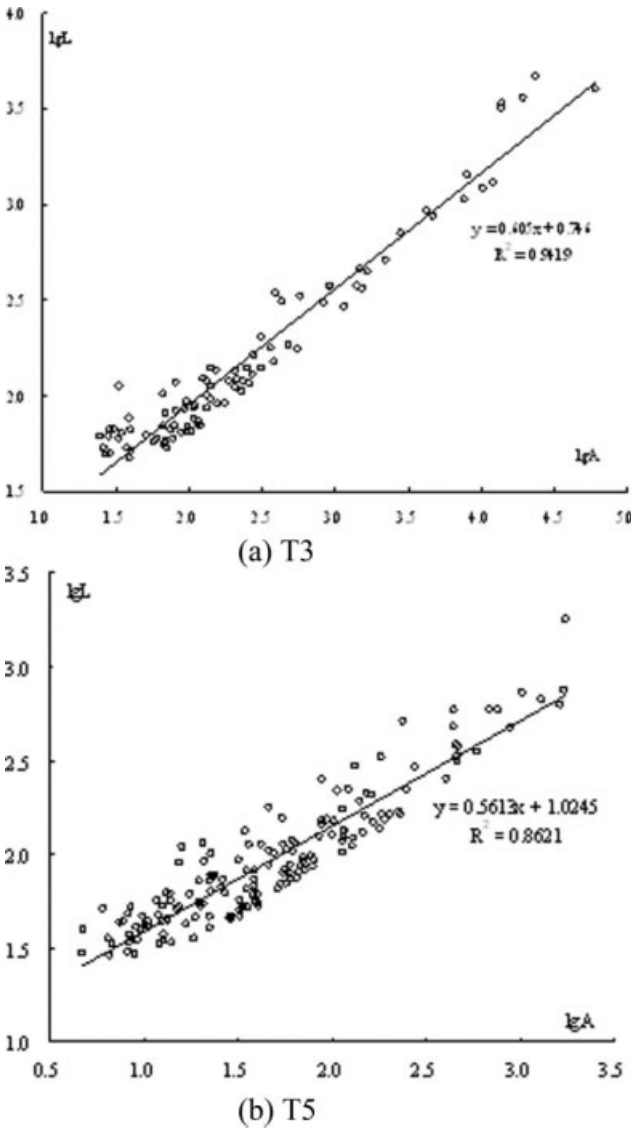

Figure 10 Calculation of fractal dimension of pore boundary of hydrogel after repeated water absorption and water release.

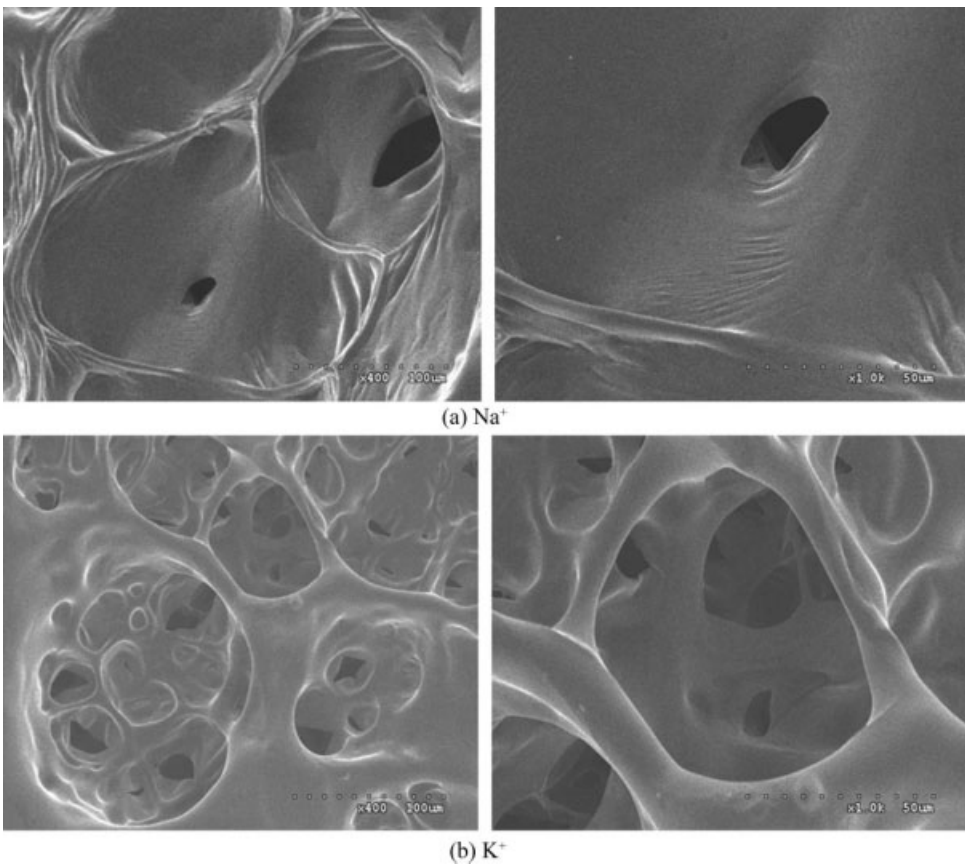

Figure 11 Micromorphology of HLM after swelling in solutions of monovalent cation.

absorption velocity of KH is larger than that of AS, and water absorption velocity of AS is larger than that of HLM. The scanning results of micromorphology of dry gel particles of the three types of SAP indicate that there are pores on the surface of KH and water molecules that can pass through these pores to provoke early swelling equilibrium. There is a striation distribution on the surface of dry gel particles of HLM, and then water reaches its internal part by capillarity and the time for swelling equilibrium to occur is longer. Substantial theoretical analyses and experimental researches prove that ionic SAP has higher water absorption multiplying factor and lower water absorption velocity, whereas nonionic SAP has lower water absorption multiplying factor and higher water absorption velocity. KH is one type of ionic SAP whereas HLM is one type of nonionic SAP. The experiment in this article confirms that KH has higher water absorption multiplying factor and lower water absorption velocity. The time for reaching its water absorption equilibrium is 180 min. HLM has lower water absorption multiplying factor and higher water absorption velocity. The time for reaching its water absorption equilibrium is 84.0 min. The results of swelling characteristic curves of the three types of SAP are indicated as follows: during the initial phase, water absorption velocity of KH is the highest whereas that of HLM is the lowest; for the middle phase, the sequence is just on the contrary. The primary reason for this phenomenon to occur is that SAP is a high polymer with various hydrophilic groups and a low crosslinking degree. During the initial phase, water absorption occurs by capillarity and diffusion on the surface of particles. The hydrogel formed prevents further penetration of water into the internal part of SAP particles. This process is mainly controlled by the superficial micromorphology of dry gel particles. The swelling process is mainly controlled by the diffusion of crosslinking network of SAP in water solution. Water absorption by ionic SAP relies on osmotic pressure, whereas water absorption by nonionic SAP relies on the hydrophilic interaction of hydrophilic groups. Hence, the nonionic SAP has higher diffusion capacity and water absorption velocity is larger.

The issue of repeated water absorption and water release property and its mechanism is important for the application of SAP in agriculture and gardening. This work discovers that the swelling multiplying factor of HLM in deionized water abides by an "inverted U" distribution. The swelling multiplying factor increases over the first three tests and then decreases. Water absorption multiplying factor for

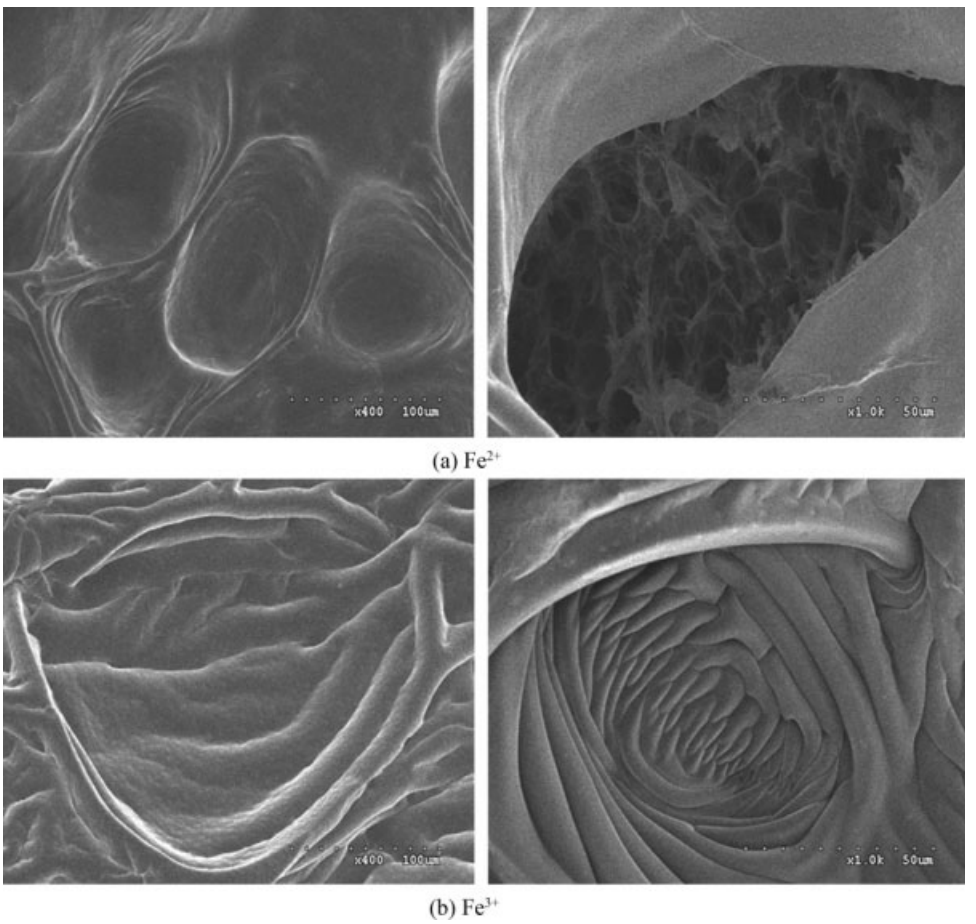

Figure 12 Micromorphology of HLM after swelling in solutions of higher-valent cation.

the third test is the largest one. Water absorption capacity of SAP is decided by both the extension caused by ionic charge repulsion of macromolecular ionic charges and the expansion resistance caused by crosslinking network. With the increase of number of times of repeated water absorption and water release, the elastic modulus of crosslinking network and its stretch and recovery also reduce. Thus, the water absorption multiplying factor increases with respect to the increase of number of times of repeated water absorption and water release. On the other hand, there exists a superficial dissolution phenomenon during the swelling process of SAP.[13] The molecules on outermost layer of SAP may have been turned into the gel and may have been scattered into the solvent. With ESEM, it is discovered that the physical structure of HLM hydrogel after repeated water absorption and water release transfers from gridding membrane structure to network structure. The rupture of membrane structural matter means that it is easier for network frame to rupture and for SAP to dissolve. With the increase of number of times of repeated water absorption and water release, the amount dissolved increases and the amount of dry matter reduces. In practical operation, it is hard to calculate the amount dissolved, and the amount of dry matter is assumed to be the same as its initial value (commonly 1.0 g), and thus the calculated water absorption multiplying factor is lower than its real value. These two kinds of factors cause the swelling multiplying factor of HLM in deionized water abiding by an "inverted U" distribution.

With ESEM, research results of superficial micromorphology of SAP hydrogel indicate that hydrogel possesses a network frame with many pores of different sizes and shapes and it also possesses property of self-similarity, fine structure, and fractal characteristics. The pore cross-sectional boundary, pore size, and distribution are important characteristic parameters to describe and represent micromorphology of pores. The shape of cross-sectional boundary of pores can describe the regularity property of pores. The perimeter of pores with a certain area can reflect the geometric property of pores. The longer the perimeter of cross-section of pore, the larger is the tortuosity of pore boundary, and the same are the irregularity of geometric shape of pore and the fractal dimension. With the increase of number of times of repeated water absorption and water

release, the stretch and recovery of crosslinking network of SAP reduce. The pore boundary becomes smoother and smoother, and the resistance to water flow in pores reduces. Thus, water absorption velocity, water absorption multiplying factor, and fractal dimension of pore boundary increase with respect to the increase of the number of times of repeated water absorption and water release. The influence of various cations on the micromorphology of hydrogel is diverse and the fractal property does not exist. The introduction of various cations increases the number of crosslinking points in molecules and causes the occurrence of entanglement within gel structure.

Although this work shows the quantitative analysis for micromorphology of SAP with ESEM and fractal theory, it is still urgent to conduct researches on nonuniformity, pore sizes, and fractal characteristics at different levels for internal pore structure of hydrogel.

CONCLUSIONS

Four categories of conclusions have been achieved based on this research:

1. During the initial phase, water absorption velocity of KH is the highest while that of HLM is the lowest. This process is mainly controlled by superficial micromorphology of dry gel particles. During the middle phase, water absorption velocity of KLM is the highest while that of KH is the lowest. This process is mainly controlled by the diffusion of crosslinking network of SAP in water solution.
2. After removal of ionic water, KH hydrogel possesses a classical alveolate crosslinking network structure. HLM hydrogel possesses a crosslinking gridding membrane structure, and AS hydrogel possesses a transitional one between gridding membrane and network structure. Various cation solutions affect the micromorphology of hydrogel and both uniqueness and diversity prevail. The introduction of various cations increase the number of crosslinking points in molecules and causes the occurrence of entanglement within the gel structure.
3. Under the condition of repeated water absorption and water release, swelling multiplying factor of HLM in deionized water abides by an "inverted U" distribution. Water absorption multiplying factor for the third test is the largest one. This is primarily caused by both reduction of resilience of crosslinking network and dissolution of polymer on the surface of hydrogel.
4. The network boundary of pores of the three types of SAP hydrogels possesses fractal characteristics, and fractal dimensions are from 1.35 to 1.65. The fractal dimension of HLM is smaller than that of AS while that of KH is the largest. With the increase of number of times of repeated water absorption and water release, the fractal dimension of cross-sectional pore boundary reduces, that is, T1 (1.3848) $>$ T3 (1.2100) $>$ T5 (1.1226).

References

1. Abedi-Koupaic, J.; Sohrab, F.; Swarbrick, G. J Plant Nutr 2008, 31, 317.
2. Chen, Y.; Tan, H. Carbohydr Res 2006, 341, 887.
3. Jurjiu, A.; Koslowski, T.; Von Ferber, C.; Blumen, A. Chem Phys 2003, 294, 187.
4. Raju, K. M.; Raju, M. P. Adv Polym Technol 2001, 20, 146.
5. Masaro, L.; Zhu, X. X. Prog Polym Sci 1999, 24, 731.
6. Schott, H. J Macromol Sci Phys B 1992, 31, 1.
7. Lee, W. F.; Fu, Y. T. J Appl Polym Sci 2003, 89, 3652.
8. Xu, C.; Breedveld, V.; Kopecek, J. Biomacromolecules 2005, 6, 1739.
9. Kishi, R.; Kihara, H.; Miura, T. Colloid Polym Sci 2004, 283, 133.
10. Stanley, H. E.; Meakin, P. Nature 1988, 335, 405.
11. Liu, G.; Wan, Z.; Jin, Y. Polym Mater Sci Eng 2002, 18, 26.
12. Posadas, A. N. D.; Giménez, D.; Quiroz, R. Soil Sci Soc Am J 2003, 67, 1361.
13. Lin, X.; Li, Y.; Xu, T.; Yang, P.; Ren, S. Polym Mater Sci Eng 2008, 24, 116.